Broad antifungal resistance mediated by RNAi-dependent epimutation in the basal human fungal pathogen *Mucor circinelloides*

Zanetta Chang[1], R. Blake Billmyre[2], Soo Chan Lee[3], and Joseph Heitman[1,*]

[1]Department of Molecular Genetics and Microbiology, Duke University, Duke University Medical Center, Durham, North Carolina, United States of America

[2]Stowers Institute for Medical Research, Kansas City, Missouri, United States of America

[3]South Texas Center for Emerging Infectious Diseases (STCEID), Department of Biology, University of Texas, San Antonio, San Antonio, Texas, United States of America

[*]Corresponding author:

Email: heitm001@duke.edu (JH)

Abstract

Mucormycosis - an emergent, deadly fungal infection - is difficult to treat, in part because the causative species demonstrate broad clinical antifungal resistance. However, the mechanisms underlying drug resistance in these infections remain poorly understood. Our previous work demonstrated that one major agent of mucormycosis, Mucor circinelloides, can develop resistance to the antifungal agents FK506 and rapamycin through a novel, transient RNA interference-dependent mechanism known as epimutation. Epimutations silence the drug target gene and are selected by drug exposure; the target gene is re-expressed and sensitivity is restored following passage without drug. This silencing process involves generation of small RNA (sRNA) against the target gene via core RNAi pathway proteins. To further elucidate the role of epimutation in the broad antifungal resistance of Mucor, epimutants were isolated that confer resistance to another antifungal agent, 5-fluoroorotic acid (5-FOA). We identified epimutant strains that exhibit resistance to 5-FOA without mutations in PyrF or PyrG, enzymes which convert 5-FOA into the active toxic form. Using sRNA hybridization as well as sRNA library analysis, we demonstrate that these epimutants harbor sRNA against either *pyrF* or *pyrG*, and further show that this sRNA is lost after reversion to drug sensitivity. We conclude that epimutation is a mechanism capable of targeting multiple genes, enabling Mucor to develop resistance to a variety of antifungal agents. Elucidation of the role of RNAi in epimutation affords a fuller understanding of mucormycosis. Furthermore, it improves our understanding of fungal pathogenesis and adaptation to stresses, including the evolution of drug resistance.

Author Summary

The emerging infection mucormycosis causes high mortality in part because the major causative fungi, including *Mucor circinelloides,* are resistant to most clinically available antifungal drugs. We previously discovered an RNA interference-based resistance mechanism, epimutation, through which *M. circinelloides* develops transient resistance to the antifungal agent FK506 by altering endogenous RNA expression. We further characterize this novel mechanism by isolating epimutations in two genes that confer resistance to another antifungal agent, 5-fluoroorotic acid. Thus, we demonstrate epimutation can induce resistance to multiple antifungals by targeting a variety of genes. These results reveal epimutation plays a broad role enabling rapid and reversible fungal responses to environmental stresses, including drug exposure, and controlling antifungal drug resistance and RNA expression. As resistance to antifungals emerges, a deeper understanding of the causative mechanisms is crucial for improving treatment.

62 # Introduction
63

64 Mucormycosis, an emerging fungal infection, is notable for very high mortality,
65 ranging from 50% for rhino-orbital-cerebral infections to 90% in disseminated infections
66 [1]. Mucormycosis primarily affects immunocompromised patients: most commonly
67 patients with diabetes, followed by those with hematologic cancers, prior organ
68 transplants, trauma, and iron overload disorders [2, 3]. The increasing prevalence of
69 these immunosuppressive disorders may explain the rising incidence of mucormycosis.
70 Another major problem is that treatment options are very limited, with first-line therapy
71 consisting of surgical debridement combined with amphotericin B or isavuconazole, the
72 only FDA-approved antifungal agents for mucormycosis [4-6]. Even after recovery
73 patients often suffer from permanent disfigurement.
74

75 The etiologic causes of mucormycosis are the Mucoralean fungi, of which the three
76 most common infectious genera are *Rhizopus, Mucor,* and *Lichtheimia* [7]. Of these
77 genera, *Mucor* has served as a model organism in various aspects of fungal biology (e.g.
78 RNAi biology, virulence, and light sensing), and the scientific community has developed
79 a set of tools for genetic manipulation [8-12]. Despite this knowledge base, many gaps
80 remain in our understanding of the pathogenesis of *Mucor* as well as the biology of all
81 Mucoralean species. For example, the broad, intrinsic antifungal resistance common to
82 Mucoralean fungi results in limited treatment options and may contribute to the high
83 mortality associated with mucormycosis, yet the mechanisms underlying this resistance
84 remain largely uncharacterized. Our laboratory previously identified a form of drug

85 resistance in *Mucor* that is dependent upon endogenous RNA interference (RNAi),
86 referred to as epimutation [13, 14].
87
88 RNAi is a mechanism that targets specific mRNA transcripts and inactivates them
89 through either mRNA degradation or inhibition of translation. The first description of RNAi
90 in fungi was quelling, a mechanism for silencing repetitive sequences and transposons in
91 the model fungus *Neurospora crassa* [15]. Later, RNAi was fully characterized in the
92 nematode *Caenorhabditis elegans* [16], and has since been shown to be conserved
93 throughout many eukaryotic lineages including a variety of fungi [17]. Many other forms
94 of RNAi have since been characterized in fungi, including meiotic silencing by unpaired
95 DNA in *Neurospora*, sex-induced silencing in *Cryptococcus neoformans*, and
96 heterochromatin formation in *Schizosaccharomyces pombe* [18-21]. RNA-based control
97 of fungal drug sensitivity was previously described in *S. pombe,* where a long non-coding
98 RNA has been shown to epigenetically repress transcription of a permease and,
99 therefore, decrease global drug sensitivity [22]. However, no RNAi-mediated form of drug
100 resistance was described prior to our previous finding of epimutation in *Mucor* [13, 14]. In
101 the Mucoralean fungi, RNAi machinery is conserved and functions to trigger silencing in
102 *Mucor circinelloides* and *Rhizopus delemar/Rhizopus oryzae* [8, 23, 24]. Thus, *Mucor*
103 serves as a model fungus for the study of RNAi and epimutation.
104
105 The novel mechanism of epimutation involves the intrinsic RNAi silencing pathway,
106 which transiently suppresses expression of fungal drug target genes. Epimutants in
107 *Mucor* were previously identified that confer resistance to the antifungal agents FK506

and rapamycin. These epimutants harbor antisense small RNAs (sRNA) specific to the *fkbA* gene that trigger mRNA degradation and thereby prevent production of the drug target FKBP12 [13]. Epimutation is transient; after passage without FK506 drug selection, mRNA expression recovered gradually until *fkbA* mRNA returned to wild-type expression levels and, conversely, expression of the *fkbA*-specific sRNA was lost. Epimutation in *Mucor* requires multiple canonical RNAi proteins, including Dicer (Dcl1 and Dcl2), Argonaute (Ago1), and RNA-dependent RNA polymerase (RdRP2). Deletion of genes encoding these RNAi components in *M. circinelloides* led to an inability to form epimutants, showing that epimutation is dependent upon the RNAi pathway. Interestingly, deletion of two other RNA-dependent RNA polymerases, RdRP1 or RdRP3, or the RNAi pathway component R3B2, led to a significantly higher rate of epimutation, suggesting these components play an inhibitory role [14]. Taken together, these findings reveal the intrinsic RNAi pathway in *Mucor* can suppress drug target expression in a reversible fashion.

We report here the identification of epimutants resistant to an additional antifungal, the laboratory agent 5-fluoroorotic acid (5-FOA). 5-FOA is converted into a toxin by action of orotate phosphoribosyltransferase (PyrF) and orotidine-5'-monophosphate decarboxylase (PyrG), two enzymes in the uracil biosynthetic pathway. Antifungal resistance is evoked by selective generation of sRNA against either *pyrF* and *pyrG*. Similar to previous observations with FK506-resistant epimutants, sRNA generation in 5-FOA-resistant epimutants is transient and lost after passage in the absence of drug selection, or when the epimutants are grown in conditions lacking uracil. These

observations build on our prior findings to establish that epimutation is a general phenomenon that can affect multiple genetic loci in *Mucor* and induce resistance to multiple antifungal agents. The transient nature of epimutation allows for rapid adaptation through generation of phenotypic diversity in response to a variety of stresses, such as drug stress or auxotrophy. These findings advance our understanding of the genetic and molecular basis for antimicrobial drug resistance with implications for other pathogenic microbes with active RNAi pathways.

Results

Epimutation induces transient resistance to 5-FOA

Our previous work identified epimutation as a novel mechanism of antifungal resistance, but we had only studied sRNAs generated against a single locus, *fkbA* [13]. To determine the broader scope epimutation might play in *Mucor* drug resistance, we generated epimutations against another antifungal compound. The well-characterized laboratory antifungal agent 5-fluoroorotic acid (5-FOA) possesses efficacy against *Mucor* and is used as a tool for genetic manipulation [12, 25-27]. The genes responsible for 5-FOA toxicity in *Mucor* encode orotate phosphoribosyltransferase (*pyrF*) and orotidine-5'-monophosphate decarboxylase (*pyrG*) [28, 29]. PyrF and PyrG are responsible for the conversion of 5-FOA, a prodrug, into 5-fluorouracil, which serves as a toxic nucleotide analog. Therefore, a loss-of-function mutation in either of these two genes confers resistance. Because these genes also play roles in the pyrimidine synthesis pathway, *pyrF* or *pyrG* mutation also causes uracil auxotrophy. The clear understanding of the mechanisms and targets of 5-FOA simplified the process of screening for epimutants.

To increase the possibility of isolating epimutants we performed initial screens in two RNAi-deficient backgrounds, *rdrp1*Δ and *rdrp3*Δ, which demonstrated an enhanced rate of epimutation in previous studies of FK506-resistant epimutation [14]. These *rdrp1*Δ and *rdrp3*Δ mutant strains contain two copies of *pyrG.* The original *pyrG* locus contains a known point mutation, G413A, which confers 5-FOA resistance. Due to the limited selectable markers available for *Mucor*, a functional copy of *pyrG* was subsequently inserted into either the *rdrp1* or *rdrp3* locus to generate the

RNAi mutant strains. Therefore, to sequence and identify *pyrG* mutations in RNAi mutant strains, we specifically amplified the copy of *pyrG* inserted in either *rdrp1* or *rdrp3* using the appropriate locus-specific primers (S1 Table). Of note, all of the *pyrG* mutations found in this study match the original mutation seen in the endogenous mutant *pyrG* locus (S2 Table). This is most likely due to gene conversion from the endogenous locus, indicating a higher rate of gene conversion when compared to *de novo* mutation. This phenomenon may have contributed to the relatively low frequency of isolation of *pyrG* epimutants.

To derive 5-FOA-resistant isolates, *rdrp1*Δ and *rdrp3*Δ strains were grown in the presence of 5-FOA in media supplemented with uridine and uracil. Under these conditions the strains, initially sensitive, grew as abnormal, stunted hyphae; but after approximately two weeks of incubation patches of resistant filamentous growth were isolated and analyzed. Two *pyrF* epimutants (designated as strains E1 and E2) were isolated from an *rdrp3* mutant strain. In addition, four *pyrF* epimutants (including strains E3 and E5) and one *pyrG* epimutant (E4) were isolated in an *rdrp1* mutant strain, a second strain with enhanced rates of epimutation [13]. Based on sRNA hybridization analysis, representative epimutants express antisense sRNA against either the *pyrF* or *pyrG* locus, but not both (Fig. 1a, b). No 5-FOA-resistant epimutant strains were identified in wild-type strains R7B (*M. circinelloides* f. *lusitanicus*) or 1006PhL (*M. circinelloides* f. *circinelloides*), or in an *r3b2*Δ strain, mutated for a different RNAi component (S2 Table). Interestingly, rates of 5-FOA-resistant epimutation in all strains tested were decreased compared to the rates seen in the initial report of FK506-resistant epimutants (Table 1).

Table 1. Rates of *pyrF* and *pyrG* epimutation by background strain

		Total	Epimutant	Mutant	Unknown
*rdrp3*Δ	Number of isolates	14	2	0	12
	Percentage		14.3%	0%	85.7%
*rdrp1*Δ	Number of isolates	27	5	20	2
	Percentage		18.5%	74.1%	7.4%
*r3b2*Δ	Number of isolates	14	0	12	2
	Percentage		0%	85.7%	14.3%
R7B	Number of isolates	2	0	0	2
	Percentage		0%	0%	100.0%
1006PhL	Number of isolates	61	0	28	33
	Percentage		0%	45.9%	54.1%

All epimutant strains were stably 5-FOA-resistant when maintained under drug selection conditions. However, following passage on media lacking 5-FOA, all five strains reverted to a 5-FOA sensitive phenotype. To determine 5-FOA sensitivity, epimutant and passaged strains were plated on MMC media without uracil, MMC with uracil supplementation, and MMC with 5-FOA and uracil for phenotypic analysis (Fig. 1c, d). Uracil auxotrophic strains with known mutations, such as the *pyrG*- mutant strain, are unable to grow robustly on MMC alone. In contrast, the epimutant strains were able to grow to some extent on MMC. Epimutant E2 shows qualitatively reduced growth on agar plates relative to the parental strain, while epimutant E4 shows growth indistinguishable from the parental strain. This suggests that epimutants placed in auxotrophic conditions may still be able to synthesize uracil at a low level; or, alternatively, that the epimutation has begun to revert toward wild-type when epimutant spores are incubated on MMC. Complete reversion of epimutant strains - loss of 5-FOA resistance and wild-type rates of growth on MMC - was observed for *pyrF* epimutants E1, E3, and E5, as well as *pyrG* epimutant E4 after five passages (Fig. 1d). The *pyrF* epimutant E2 demonstrated only

partial reversion to drug sensitivity after five passages but complete reversion after ten (Fig. 1c). sRNA was isolated from these reverted strains after five or ten passages and sRNA hybridization was performed. Strains E1, E3, E4, and E5 demonstrated a complete loss of *pyrF* or *pyrG* sRNA after five passages, corresponding with their phenotypic reversion; likewise, strain E2 demonstrated a reduction of *pyrF* sRNA after five passages and complete loss after ten passages (Fig. 1a, b).

5-FOA-resistant epimutants express sRNA specific to the *pyrF* or *pyrG* locus

sRNA libraries were generated from *pyrF* epimutants (E1, E2) and the *pyrG* epimutant (E4) as well as their corresponding revertants, and these libraries were sequenced via Illumina. Epimutation induced a significant increase in both sense and antisense sRNAs against *pyrF* or *pyrG* in their respective epimutants. For *pyrF*, which contains no introns, these sRNAs were distributed across the ORF (Fig. 2a). sRNAs expressed against *pyrG* were localized specifically to the exons (Fig. 2b). In both cases, these sRNAs are homologous to the target loci and not to either upstream or downstream regions. Genome-wide, *pyrF* and *pyrG* were among the genes most strongly differentially enriched for sRNAs in the epimutant versus the revertant strains, even without complete reversion to wild-type levels in the revertants (S1 Fig). Expression of the *pyrF* or *pyrG* specific sRNAs was lost upon reversion to 5-FOA sensitivity, although the E1 revertant did not return completely to parental levels after five passages.

***pyrF* and *pyrG* epimutants harbor sRNAs with characteristic features**

sRNAs from 5-FOA-resistant *pyrF* or *pyrG* epimutants also shared characteristics typical of sRNAs involved in the canonical RNAi pathway. These features included a high

prevalence of a 5' terminal uracil, which was found in antisense sRNAs in particular (Fig. 3a, 3b). Representative analysis from the *pyrF* epimutant E1 is shown here (Fig. 3a), as well as from the *pyrG* epimutant E4 (Fig. 3b). The same 5' uracil predominance was observed in the few antisense sRNA reads found in the revertants; for better visualization a version of this figure with a scaled Y-axis has also been included (S2 Fig). This 5' uracil prevalence was not identified in sense sRNAs from the same regions. In addition, the lengths of sRNA molecules homologous to these loci were predominantly between 21 and 24 nucleotides (Fig. 3c, 3d), a second feature of sRNAs generated by the canonical RNAi pathway and which interact with the RNAi effector protein Argonaute.

A subset of genes with similarity to transposons exhibits altered sRNA levels

Analysis of genome-wide sRNA content also revealed a subset of genes that behaved unexpectedly in different samples. This set of genes had reduced sRNA content in the E2 epimutant, an *rdrp3*Δ mutant, compared to the rest of the *rdrp3*Δ strains that were sequenced (S3 Fig). Interestingly, while sRNA levels of these genes in the wild-type parent of the *rdrp1*Δ mutant were similar to levels in the *rdrp3*Δ mutant and its wild-type parent, all three sequences of *rdrp1*Δ strains in this study had lower sRNA levels corresponding to the same set of genes that behaved unusually in the E2 revertant (S3 Fig). A cutoff of 15-fold enrichment in the E4 revertant over the E4 epimutant was established, which selected 516 genes. Analysis of this gene set was complicated by generally low quality functional annotation of the *Mucor* genome. These genes were not grouped in any genomic location region but were relatively evenly distributed, appearing on every scaffold of the genome over 41 kb in size (S3 Fig). A search for conserved

domains in this gene set revealed only 152 genes that encoded identifiable functional domains. However, 91 of these genes had predicted functions consistent with transposons or retrotransposons, including reverse transcriptase or transposase domains. These results may suggest that RdRP1 plays a role in repressing transposable elements via sRNA. However, the aberrant behavior of the E2 epimutant is not explained by this hypothesis because both the epimutant and its revertant are in the *rdrp3*Δ background. This suggests another level of regulation of this unusual class of sRNA.

Epimutants exhibit reduced expression of target genes

Analysis of *pyrF* and *pyrG* mRNA expression levels by quantitative real-time PCR (qRT-PCR) showed a decrease in expression levels in epimutant isolates corresponding with sRNA generation. In *pyrF* epimutant strains, expression of *pyrF* mRNA was significantly decreased relative to expression in the *rdrp3* mutant parental background. Moreover, *pyrF* expression levels were restored upon reversion of the *pyrF* epimutation after five or ten passages (Fig. 4 a). As expected, no significant decrease was observed in *pyrG* expression in these *pyrF* epimutants either before or after reversion (Fig. 4b). Correspondingly, in the *pyrG* epimutant strain, decreased expression of *pyrG* but not *pyrF* mRNA was observed, with a subsequent increase upon reversion to 5-FOA sensitivity (Fig. 4 c, d).

Discussion

Epigenetic alteration of gene expression can lead to marked changes in phenotype across a variety of organisms. The phenomenon of epimutation was first described in plants and later in cancer biology; these particular alterations are attributable to extensive DNA methylation leading to gene silencing. Epimutations in snapdragons produce a phenotype wherein normal floral bilateral asymmetry is converted to radial symmetry [30]. In the field of cancer research, there is growing awareness that carcinogenesis can be driven by epimutation rather than mutations, including but not limited to cancers such as hereditary nonpolyposis colorectal cancer or BRCA-associated breast cancer [31-35]. Another role of epimutation that has gained attention is as a mechanism of drug resistance, with a particular focus on the roles played by DNA methylation and long noncoding RNAs in tumor drug resistance [36, 37]. Finally, a third form of epigenetic drug resistance, RNAi-dependent epimutation, was discovered to be a novel and transient mechanism of resistance to the agent FK506 in pathogenic fungi [13].

Identification of 5-FOA-resistant *Mucor* epimutants confirms that this mechanism is broader than had been previously demonstrated. Epimutation is capable of conferring resistance to multiple antifungal agents with different mechanisms of action, by targeting multiple genes. 5-FOA-resistant epimutant strains were identified that demonstrated silencing of either the *pyrF* locus or the *pyrG* locus. Therefore, generalization of the mechanism suggests that epimutation may broadly contribute to resistance by silencing a variety of drug target genes. No specific triggers for RNAi-based epimutation have been identified to date, although various stress conditions were previously tested [13]. The

293 previous locus of epimutation, *fkbA*, was noted to have an overlapping gene (*patA*), but
294 deletion of *patA* did not cause a loss of epimutation [13]. *pyrF* and *pyrG* do not have any
295 overlapping flanking genes.
296
297 Rapid loss of silencing was observed in 5-FOA-resistant epimutant strains after
298 five to ten passages without drug selection pressure. Epimutation – a transient and
299 reversible phenomenon – may provide multiple advantages over genetic mutations that
300 stably alter DNA sequence. In *Mucor*, which is aseptate and multinucleate, RNA-based
301 silencing may induce more rapid and complete loss of function of disadvantageous genes
302 compared to a recessive nuclear mutation, which would be required to sweep the
303 population to become homokaryotic. In addition, the reversible nature of epimutation
304 allows for subsequent reversal of adaptations that may be disadvantageous after a
305 selective pressure is no longer present. For example, the uracil auxotrophy induced
306 secondary to 5-FOA resistance could affect growth in low uracil conditions; under such
307 conditions, epimutants, which can rapidly revert to wild-type and resume uracil synthesis,
308 would have an advantage over *pyrF* or *pyrG* mutants. In support of this hypothesis we
309 observed that *pyrF* and *pyrG* epimutants grew more effectively than a *pyrG* mutant strain
310 in MMC lacking uracil supplementation, indicating that the epimutants may have
311 incompletely silenced the *pyrF* or *pyrG* gene or may be undergoing reversion in response
312 to selective pressure (Fig. 1). This is further supported by our qPCR data that
313 demonstrated reduced, but not abolished, levels of *pyrF* or *pyrG* expression in the
314 respective epimutants (Fig. 4).

315 The phenomenon of epimutation could thus be comparable to other described
316 instances of fungal epigenetic heterogeneity, serving as a bet-hedging strategy that
317 enables rapid and reversible responses to a variety of environmental conditions. One
318 previously described example is telomeric silencing: genetic markers located near the
319 telomeres of *S. cerevisiae*, including *URA3* as well as *ADE2*, were demonstrated to be
320 variably silenced in a given population of yeast [38, 39]. These mixed populations
321 (*URA*$^{+}$*/ura*$^{-}$ or *ADE*$^{+}$*/ade*$^{-}$) are attributable to telomeric heterochromatin expanding and
322 contracting across the integrated gene, resulting in silencing or expression. Likewise, in
323 the fungal pathogen *C. neoformans*, the phenomena of sex-induced silencing or mitotic-
324 induced silencing can be observed after tandem insertions of transgenes such as *ADE2*.
325 The variable silencing of this tandem array can be observed through the phenomenon of
326 variegation of colonies with both *ADE* and *ade*- phenotypes [19, 21, 40].
327
328 *Mucor* is known to possess multiple functional RNAi pathways [9, 41]. The sRNAs
329 generated from the *pyrF* and *pyrG* loci show hallmark properties of RNAs that induce
330 silencing through the core RNAi pathway [41]. Furthermore, sRNAs from *pyrG* localized
331 to the exons of these genes, suggesting that the sRNAs were most likely generated and
332 processed from mature mRNA. The gene *pyrF* contains no introns, but sRNAs were found
333 to localize across the entire open reading frame without extending into neighboring
334 regions. This suggests introns are not required for epimutation, and thus epimutation is
335 distinct from previously described mechanisms of RNAi-mediated degradation that target
336 poorly spliced introns [42].
337

5-FOA-resistant epimutants were discovered in two distinct genetic backgrounds: the *rdrp1* and *rdrp3* mutants, each of which lacks one of the three RNA-dependent RNA polymerases with roles in RNAi in *Mucor*. However, unlike the previous report of FK506-resistant epimutants, no 5-FOA-resistant epimutant strains were identified in wild-type strains or in an *r3b2*Δ strain mutated for a different RNAi component (S2 Table). In both the *rdrp1* and *rdrp3* mutant backgrounds, the overall frequency of 5-FOA-resistant epimutants was notably lower than the frequency of FK506-resistant epimutants, potentially due to the auxotrophic effect caused by loss of *pyrF* or *pyrG*. These RNAi deficient strains were previously demonstrated to have an increased frequency of epimutation relative to wild-type [13, 14]. Hence, one possibility is that the frequency of wild-type epimutants resistant to 5-FOA may be even lower that the frequency seen in RNAi mutant strains, making these wild-type epimutants difficult to isolate. Alternatively, it is possible that these mutant backgrounds are required for the isolation of 5-FOA-resistant epimutants. If RNAi deficiency is required for generation of 5-FOA-resistant epimutants, these findings would illustrate an interesting potential pathway to drug resistance that combines both a Mendelian (*rdrp1*Δ or *rdrp3*Δ) and an epigenetic factor in a two-step process.

Epimutation may enable an organism to temporarily resist environmental stresses to provide time for more permanent genetic diversity to arise. For example, induction of drug tolerance has been shown to play a role in subsequent mutation and the eventual development of bona fide drug resistance in bacteria [43, 44]. Similarly, aneuploidy has been reported to serve as a transient evolutionary adaptation that enables other genetic

361 changes to arise [45]. One 5-FOA-resistant strain generated in this study, epimutant E7,
362 initially expressed sRNA against *pyrF* and had no mutations in *pyrF* or *pyrG*. It lost this
363 sRNA expression by passage 15, but did not revert to 5-FOA sensitivity even after 70
364 passages without selection (S4 Fig). Neither *pyrF* nor *pyrG* mutations were identified in
365 this strain after passaging. One potential explanation based on these results is that
366 epimutation provided transient relief from drug toxicity for this isolate and thus enabled
367 the development of a more permanent form of resistance that remains to be elucidated.
368
369 In broader clinical terms, it is interesting to consider the role epimutation may play
370 in *Mucor's* intrinsic resistance to many antifungal agents, and whether epimutation may
371 affect development of further resistance. For example, it has been suggested that amino
372 acid substitutions in the *Mucor* Erg11/CYP51 enzyme, the target of the azole drug class,
373 may explain part of *Mucor*'s innate resistance to certain structural classes of azoles (i.e.
374 short- vs long-tailed azoles) [46]. However, this distinction alone is not sufficient to explain
375 why only two azoles possess efficacy against *Mucor,* and additional mechanisms for
376 intrinsic azole resistance should be investigated. In addition, epimutation could play a role
377 in development of resistance to effective antifungals. The two front-line antifungals in
378 clinical use against mucormycosis are the azole isavuconazole and the polyene
379 amphotericin B. Resistance to azoles and polyenes in other pathogenic fungi, such as
380 *Candida* species, can be mediated by loss of the ergosterol biosynthetic enzymes Erg3
381 and Erg6 [47-52]. Using bioinformatic analysis we have identified three candidate *ERG6*
382 homologs and one candidate *ERG3* homolog in *Mucor* and we hypothesize that
383 epimutation could induce silencing of these genes under appropriate drug selection,

leading to acquired drug resistance. In particular, the presence of multiple copies of the gene encoding Erg6 could make this enzyme an especially appealing target for epimutation; if there is sufficient homology between these copies, we hypothesize RNAi could induce silencing of all three copies at once, instead of requiring mutations at all three loci to develop resistance.

Identification and characterization of 5-FOA resistance via RNAi-based epimutation advances understanding of the general mechanisms of drug resistance in *Mucor circinelloides*. The transient nature of epimutation is advantageous as it allows for rapid, facile reversion and flexible responses to changing conditions, such as uracil auxotrophy versus drug stress, enabling better adaptation to stressful conditions. Further questions that remain include whether RNAi-based epimutation occurs in other fungal species or other organisms with active RNAi systems. Further elucidation of the mechanism of epimutation advances our understanding of RNAi, drug resistance, and stress response mechanisms and may offer novel approaches to combat antifungal drug resistance.

Materials and Methods

Strains and growth conditions

All epimutants in this study were generated from strains of *Mucor circinelloides* forma *lusitanicus*. *M. circinelloides* f. *lusitanicus* RNAi mutant strains MU439, MU440, and MU500 (independently derived strains with the genotype *leuA- pyrG- rdrp3*Δ::*pyrG*) and MU419 (*leuA- pyrG- rdrp1*Δ::*pyrG*) were previously generated from the uracil and leucine auxotrophic strain MU402, which was in turn derived from the wild-type strain CBS277.49 [13, 14, 26]. As these four RNAi mutant strains were generated by using a functional copy of the *pyrG* gene to interrupt the target RNAi gene, each strain contains a mutant, nonfunctional copy of *pyrG* at the original locus as well as a functional copy inserted in an RNAi component gene. MU439, MU419, and the wild-type strain R7B served as controls for *M. circinelloides* f. *lusitanicus* studies, as appropriate. The strain 1006PhL was used for all *M. circinelloides* f. *circinelloides* studies.

Strains were grown at room temperature (approximately 24°C) with light exposure. Strains were cultured on MMC media at pH=4.5 (10 g/L casamino acids, 20 g/L glucose, and 0.5 g/L yeast nitrogen base without amino acids or ammonium sulfate) [26]. Media was supplemented with both uridine (0.061 g/L) and uracil (0.056 g/L) for potentially auxotrophic strains. 5-FOA selection was performed on MMC plates supplemented with uracil/uridine and 2.5 mg/mL 5-FOA. Passages were performed in liquid YPD (10 g/L yeast extract, 20 g/L peptone, 20 g/L dextrose) and on YPD agar.

Generation and phenotypic analysis of 5-FOA-resistant mutants and epimutants

Epimutant candidates were generated by spotting *Mucor* spores on MMC media supplemented with 5-FOA and uridine/uracil; plates were incubated for approximately two weeks or until patches of resistant hyphal growth emerged from the periphery of drug-sensitive colonies, which were identified as colonies with severely stunted hyphae. Resistant isolates were passaged for at least two rounds of vegetative growth and sporulation under 5-FOA selection prior to sRNA analysis, to ensure a high proportion of drug resistance in the mycelia.

Epimutant strains were passaged in liquid YPD media without drug selection to induce reversion. For the first passage, spores were added to 3 mL of media and grown overnight at 30°C with shaking at 250 rpm. Subsequent passages were performed using a sterile wooden stick to break off a small portion of mycelia for transfer to fresh media. The final passage was performed using a sterile wooden stick to break off a small portion of mycelia that was placed on a YPD plate without drug selection; the plate was then incubated at room temperature (~24°C) with light to allow for growth and sporulation. Spores were collected in sterile water for subsequent analyses.

Nucleic acid extractions

Isolates were grown on MMC media, pH=4.5, supplemented with 2.5 mg/mL of 5-FOA and uridine/uracil as needed. DNA was extracted from hyphae using the MasterPure Yeast DNA Purification Kit (Epicenter Biotechnologies, Madison, WI), with the preliminary step of adding ~100 µL of 425-600 µm glass beads and vortexing for one minute to break

444 up hyphae. *pyrF* and *pyrG* were sequenced in all resistant isolates to rule out genetic
445 mutations; primers are listed in S1 Table.

446 Isolates for RNA extraction were grown on plates overlaid with sterile cellulose film
447 (ultraviolet irradiated for 10 minutes per side) to allow for easier removal of hyphae without
448 agar contamination. Small and total RNAs were extracted using the mirVana kit (Ambion,
449 Foster City, CA) for hybridization and qPCR analysis.

450

451 **sRNA hybridization**

452 For sRNA hybridization, sRNA for each sample (3.5 µg) was separated by
453 electrophoresis on 15% TRIS-urea gels, transferred to Hybond N+ filters, and cross-
454 linked by ultraviolet irradiation as previously described (2 pulses at 1.2 x 10^5 µJ per cm^2)
455 [13]. Prehybridization was carried out using UltraHyb buffer (Ambion) at 65°C. *pyrF* and
456 *pyrG* antisense-specific and 5s rRNA probes were prepared by *in vitro* transcription using
457 the Maxiscript kit (Ambion); primers are listed in S1 Table. After synthesis, riboprobes
458 were treated by alkaline hydrolysis as previously described [23], to generate an average
459 final probe size of ~50 nucleotides.

460

461 **mRNA quantification**

462 Quantification of *pyrF* and *pyrG* mRNAs was performed by quantitative real-time
463 PCR. Single-stranded cDNA was synthesized using AffinityScript (Stratagene, La Jolla,
464 CA) from RNA samples treated with Turbo DNase (Ambion). cDNA synthesized without
465 the RT/RNase enzyme mixture was used as a “no-RT control” to control for contamination
466 by residual genomic DNA. Expression of target genes was measured using Brilliant III

ultra-fast SYBR green QPCR mix (Stratagene) using an Applied Biosystems 7500 Real-time PCR system. Technical triplicates were performed for all samples in each run, and three biological replicates were performed for each experiment. Gene expression levels were normalized using actin as the reference gene via the comparative ΔΔCt method. Primers are listed in S1 Table.

Statistics

One-way ANOVAs were used to determine the significance of qPCR replicates, with Tukey's Multiple Comparison Test as a post-hoc test where appropriate. All statistical analysis was performed using GraphPad Prism.

High-throughput sRNA sequencing and mapping

sRNA libraries were prepared and sequenced at the Duke Center for Genomic and Computational Biology using the Illumina TruSeq Small RNA Library Prep Kit coupled with agarose gel size selection for the miRNA library. Reads have been deposited at GEO under project accession number GSE113706.

Reads were trimmed using Trim Galore! with default settings to remove adapters [53]. Trimmed reads were then mapped to the *Mucor circinelloides* genome from the JGI using Bowtie [54, 55]. Reads mapping to gene loci were counted using Cufflinks and guided by genome annotation from the Joint Genome Institute (JGI) genome assembly [56].

Acknowledgements

We thank Anna Floyd-Averette and Shelly Clancey for technical support, and Andrew Alspaugh, Silvia Calo, Shelly Clancey, Victoriano Garre, María Isabel Navarro-Mendoza, Francisco E. Nicolás, Carlos Pérez-Arques, Shelby Priest, Cecelia Wall, Santiago Torres Martinez, and Rosa Maria Ruiz Vazquez for critical reading of the manuscript.

References

1. Roden MM, Zaoutis TE, Buchanan WL, Knudsen TA, Sarkisova TA, Schaufele RL, et al. Epidemiology and outcome of zygomycosis: a review of 929 reported cases. Clin Infect Dis. 2005;41(5):634-53. Epub 2005/08/05. doi: 10.1086/432579. PubMed PMID: 16080086.
2. Kontoyiannis DP, Marr KA, Park BJ, Alexander BD, Anaissie EJ, Walsh TJ, et al. Prospective surveillance for invasive fungal infections in hematopoietic stem cell transplant recipients, 2001-2006: overview of the Transplant-Associated Infection Surveillance Network (TRANSNET) Database. Clin Infect Dis. 2010;50(8):1091-100. Epub 2010/03/12. doi: 10.1086/651263. PubMed PMID: 20218877.
3. Petrikkos G, Skiada A, Lortholary O, Roilides E, Walsh TJ, Kontoyiannis DP. Epidemiology and clinical manifestations of mucormycosis. Clin Infect Dis. 2012;54 Suppl 1:S23-34. Epub 2012/01/25. doi: 10.1093/cid/cir866. PubMed PMID: 22247442.
4. Spellberg B, Walsh TJ, Kontoyiannis DP, Edwards J, Jr., Ibrahim AS. Recent advances in the management of mucormycosis: from bench to bedside. Clin Infect Dis. 2009;48(12):1743-51. Epub 2009/05/14. doi: 10.1086/599105. PubMed PMID: 19435437; PubMed Central PMCID: PMCPMC2809216.
5. Marty FM, Ostrosky-Zeichner L, Cornely OA, Mullane KM, Perfect JR, Thompson GR, 3rd, et al. Isavuconazole treatment for mucormycosis: a single-arm open-label trial and case-control analysis. Lancet Infect Dis. 2016;16(7):828-37. Epub 2016/03/13. doi: 10.1016/S1473-3099(16)00071-2. PubMed PMID: 26969258.
6. Kontoyiannis DP, Lewis RE. How I treat mucormycosis. Blood. 2011;118(5):1216-24. Epub 2011/05/31. doi: 10.1182/blood-2011-03-316430. PubMed PMID: 21622653; PubMed Central PMCID: PMCPMC3292433.
7. Singh N, Aguado JM, Bonatti H, Forrest G, Gupta KL, Safdar N, et al. Zygomycosis in solid organ transplant recipients: a prospective, matched case-control study to assess risks for disease and outcome. J Infect Dis. 2009;200(6):1002-11. Epub 2009/08/08. doi: 10.1086/605445. PubMed PMID: 19659439.
8. Trieu TA, Navarro-Mendoza MI, Perez-Arques C, Sanchis M, Capilla J, Navarro-Rodriguez P, et al. RNAi-based functional genomics identifies new virulence determinants in mucormycosis. PLoS Pathog. 2017;13(1):e1006150. Epub 2017/01/21. doi: 10.1371/journal.ppat.1006150. PubMed PMID: 28107502; PubMed Central PMCID: PMCPMC5287474.
9. Trieu TA, Calo S, Nicolas FE, Vila A, Moxon S, Dalmay T, et al. A non-canonical RNA silencing pathway promotes mRNA degradation in basal Fungi. PLoS Genet. 2015;11(4):e1005168. Epub 2015/04/16. doi: 10.1371/journal.pgen.1005168. PubMed PMID: 25875805; PubMed Central PMCID: PMCPMC4395119.
10. Li CH, Cervantes M, Springer DJ, Boekhout T, Ruiz-Vazquez RM, Torres-Martinez SR, et al. Sporangiospore size dimorphism is linked to virulence of *Mucor circinelloides*. PLoS Pathog. 2011;7(6):e1002086. Epub 2011/06/24. doi: 10.1371/journal.ppat.1002086. PubMed PMID: 21698218; PubMed Central PMCID: PMCPMC3116813.
11. Silva F, Torres-Martinez S, Garre V. Distinct white collar-1 genes control specific light responses in *Mucor circinelloides*. Mol Microbiol. 2006;61(4):1023-37. Epub 2006/08/02. doi: 10.1111/j.1365-2958.2006.05291.x. PubMed PMID: 16879651.

12. Garcia A, Adedoyin G, Heitman J, Lee SC. Construction of a reyclable genetic marker and serial gene deletions in the human pathogenic Mucorales *Mucor circinelloides*. G3: Genes, Genomes, Genetics. 2017. doi: 10.1534/g3.117.041095.
13. Calo S, Shertz-Wall C, Lee SC, Bastidas RJ, Nicolas FE, Granek JA, et al. Antifungal drug resistance evoked via RNAi-dependent epimutations. Nature. 2014;513(7519):555-8. Epub 2014/08/01. doi: 10.1038/nature13575. PubMed PMID: 25079329; PubMed Central PMCID: PMCPMC4177005.
14. Calo S, Nicolas FE, Lee SC, Vila A, Cervantes M, Torres-Martinez S, et al. A non-canonical RNA degradation pathway suppresses RNAi-dependent epimutations in the human fungal pathogen *Mucor circinelloides*. PLoS Genet. 2017;13(3):e1006686. Epub 2017/03/25. doi: 10.1371/journal.pgen.1006686. PubMed PMID: 28339467; PubMed Central PMCID: PMCPMC5384783.
15. Cogoni C, Irelan JT, Schumacher M, Schmidhauser TJ, Selker EU, Macino G. Transgene silencing of the *al-1* gene in vegetative cells of *Neurospora* is mediated by a cytoplasmic effector and does not depend on DNA-DNA interactions or DNA methylation. EMBO J. 1996;15(12):3153-63. PubMed PMID: WOS:A1996UV92000026.
16. Fire A, Xu S, Montgomery MK, Kostas SA, Driver SE, Mello CC. Potent and specific genetic interference by double-stranded RNA in *Caenorhabditis elegans*. Nature. 1998;391(6669):806-11. Epub 1998/03/05. doi: 10.1038/35888. PubMed PMID: 9486653.
17. Billmyre RB, Calo S, Feretzaki M, Wang X, Heitman J. RNAi function, diversity, and loss in the fungal kingdom. Chromosome Res. 2013;21(6-7):561-72. Epub 2013/11/01. doi: 10.1007/s10577-013-9388-2. PubMed PMID: 24173579; PubMed Central PMCID: PMCPMC3874831.
18. Shiu PK, Raju NB, Zickler D, Metzenberg RL. Meiotic silencing by unpaired DNA. Cell. 2001;107(7):905-16. Epub 2002/01/10. PubMed PMID: 11779466.
19. Wang X, Darwiche S, Heitman J. Sex-induced silencing operates during opposite-sex and unisexual reproduction in *Cryptococcus neoformans*. Genetics. 2013;193(4):1163-74. Epub 2013/02/05. doi: 10.1534/genetics.113.149443. PubMed PMID: 23378067; PubMed Central PMCID: PMCPMC3606094.
20. Volpe TA, Kidner C, Hall IM, Teng G, Grewal SI, Martienssen RA. Regulation of heterochromatic silencing and histone H3 lysine-9 methylation by RNAi. Science. 2002;297(5588):1833-7. Epub 2002/08/24. doi: 10.1126/science.1074973. PubMed PMID: 12193640.
21. Wang X, Hsueh Y-PP, Li W, Floyd A, Skalsky R, Heitman J. Sex-induced silencing defends the genome of *Cryptococcus neoformans* via RNAi. Genes & Development. 2010;24(22):2566-82. doi: 10.1101/gad.1970910.
22. Ard R, Tong P, Allshire RC. Long non-coding RNA-mediated transcriptional interference of a permease gene confers drug tolerance in fission yeast. Nat Commun. 2014;5:5576. Epub 2014/11/28. doi: 10.1038/ncomms6576. PubMed PMID: 25428589; PubMed Central PMCID: PMCPMC4255232.
23. Nicolas FE, Torres-Martinez S, Ruiz-Vazquez RM. Two classes of small antisense RNAs in fungal RNA silencing triggered by non-integrative transgenes. EMBO J. 2003;22(15):3983-91. Epub 2003/07/26. doi: 10.1093/emboj/cdg384. PubMed PMID: 12881432; PubMed Central PMCID: PMCPMC169057.

583 24. Gheinani AH, Jahromi NH, Feuk-Lagerstedt E, Taherzadeh MJ. RNA silencing of lactate
584 dehydrogenase gene in *Rhizopus oryzae*. J RNAi Gene Silencing. 2011;7:443-8. Epub
585 2011/07/20. PubMed PMID: 21769297; PubMed Central PMCID: PMCPMC3131675.
586 25. Boeke JD, LaCroute F, Fink GR. A positive selection for mutants lacking orotidine-5'-
587 phosphate decarboxylase activity in yeast: 5-fluoro-orotic acid resistance. Mol Gen Genet.
588 1984;197(2):345-6. Epub 1984/01/01. doi: 10.1007/bf00330984. PubMed PMID: 6394957.
589 26. Nicolás FE, Haro JP, Torres-Martínez S, Ruiz-Vázquez RM. Mutants defective in a
590 *Mucor circinelloides dicer*-like gene are not compromised in siRNA silencing but display
591 developmental defects. Fungal Genet Biol. 2007;44(6):504-16.
592 27. Lee S, Li A, Calo S, Heitman J. Calcineurin Plays Key Roles in the Dimorphic Transition
593 and Virulence of the Human Pathogenic Zygomycete Mucor circinelloides. PLoS Pathogens.
594 2013;9(9). doi: 10.1371/journal.ppat.1003625.
595 28. Velayos A, Alvarez MI, Eslava AP, Iturriaga EA. Interallelic complementation at the
596 *pyrF* locus and the homodimeric nature of orotate phosphoribosyltransferase (OPRTase) in
597 *Mucor circinelloides*. Mol Gen Genet. 1998;260(2-3):251-60. doi: DOI 10.1007/s004380050893.
598 PubMed PMID: WOS:000077435400015.
599 29. Benito EP, Diazminguez JM, Iturriaga EA, Campuzano V, Eslava AP. Cloning and
600 sequence analysis of the *Mucor circinelloides pyrG* gene encoding orotidine-5'-monophosphate
601 decarboxylase - use of *pyrG* for homologous transformation. Gene. 1992;116(1):59-67. doi: Doi
602 10.1016/0378-1119(92)90629-4. PubMed PMID: WOS:A1992JD84000009.
603 30. Cubas P, Vincent C, Coen E. An epigenetic mutation responsible for natural variation in
604 floral symmetry. Nature. 1999;401(6749):157-61. Epub 1999/09/18. doi: 10.1038/43657.
605 PubMed PMID: 10490023.
606 31. Brown R, Curry E, Magnani L, Wilhelm-Benartzi CS, Borley J. Poised epigenetic states
607 and acquired drug resistance in cancer. Nat Rev Cancer. 2014;14(11):747-53. Epub 2014/09/26.
608 doi: 10.1038/nrc3819. PubMed PMID: 25253389.
609 32. Gazzoli I, Loda M, Garber J, Syngal S, Kolodner RD. A hereditary nonpolyposis
610 colorectal carcinoma case associated with hypermethylation of the *MLH1* gene in normal tissue
611 and loss of heterozygosity of the unmethylated allele in the resulting microsatellite instability-
612 high tumor. Cancer Res. 2002;62(14):3925-8.
613 33. Esteller M, Silva J, Dominguez G, Bonilla F, Matias-Guiu X, Lerma E, et al. Promoter
614 hypermethylation and BRCA1 inactivation in sporadic breast and ovarian tumors. JNCI: Journal
615 of the National Cancer Institute. 2000;92(7):564-9. doi: 10.1093/jnci/92.7.564.
616 34. Snell C, Krypuy M, Wong E, investigators k, Loughrey MB, Dobrovic A. BRCA1
617 promoter methylation in peripheral blood DNA of mutation negative familial breast cancer
618 patients with a BRCA1 tumour phenotype. Breast Cancer Res. 2008;10(1). doi:
619 10.1186/bcr1858.
620 35. Suter CM, Martin DIK, Ward RL. Germline epimutation of MLH1 in individuals with
621 multiple cancers. Nature Genetics. 2004;36(5):497-501. doi: 10.1038/ng1342.
622 36. Pan J-J, Xie X-J, Li X, Chen W. Long non-coding RNAs and drug resistance. Asian Pac J
623 Cancer Prev. 2016;16(18):8067-73. doi: 10.7314/apjcp.2015.16.18.8067.
624 37. Easwaran H, Tsai HC, Baylin SB. Cancer epigenetics: tumor heterogeneity, plasticity of
625 stem-like states, and drug resistance. Mol Cell. 2014;54(5):716-27. Epub 2014/06/07. doi:
626 10.1016/j.molcel.2014.05.015. PubMed PMID: 24905005; PubMed Central PMCID:
627 PMCPMC4103691.

628 38. Gottschling DE, Aparicio OM, Billington BL, Zakian VA. Position effect at S. cerevisiae
629 telomeres: Reversible repression of Pol II transcription. Cell. 1990. doi: 10.1016/0092-
630 8674(90)90141-z.
631 39. Aparicio OM, Billington BL, Gottschling DE. Modifiers of position effect are shared
632 between telomeric and silent mating-type loci in S. cerevisiae. Cell. 1991;66(6):1279-87. doi:
633 10.1016/0092-8674(91)90049-5.
634 40. Wang X, Wang P, Sun S, Darwiche S, Idnurm A, Heitman J. Transgene induced co-
635 suppression during vegetative growth in *Cryptococcus neoformans*. PLoS genetics. 2012;8(8).
636 doi: 10.1371/journal.pgen.1002885.
637 41. Nicolas FE, Moxon S, de Haro JP, Calo S, Grigoriev IV, Torres-Martínez S, et al.
638 Endogenous short RNAs generated by Dicer 2 and RNA-dependent RNA polymerase 1 regulate
639 mRNAs in the basal fungus *Mucor circinelloides*. Nucleic Acids Research. 2010;38(16):5535-
640 41. doi: 10.1093/nar/gkq301.
641 42. Dumesic PA, Natarajan P, Chen C, Drinnenberg IA, Schiller BJ, Thompson J, et al.
642 Stalled spliceosomes are a signal for RNAi-mediated genome defense. Cell. 2013;152(5):957-68.
643 doi: 10.1016/j.cell.2013.01.046.
644 43. Billmyre RB, Heitman J. Genetic and epigenetic engines of diversity in pathogenic
645 microbes. PLoS Pathog. 2017;13(9):e1006468. Epub 2017/09/15. doi:
646 10.1371/journal.ppat.1006468. PubMed PMID: 28910393; PubMed Central PMCID:
647 PMCPMC5599048.
648 44. Levin-Reisman I, Ronin I, Gefen O, Braniss I, Shoresh N, Balaban NQ. Antibiotic
649 tolerance facilitates the evolution of resistance. Science. 2017;355(6327):826-30. Epub
650 2017/02/12. doi: 10.1126/science.aaj2191. PubMed PMID: 28183996.
651 45. Yona AH, Manor YS, Herbst RH, Romano GH, Mitchell A, Kupiec M, et al.
652 Chromosomal duplication is a transient evolutionary solution to stress. Proc Natl Acad Sci.
653 2012;109(51):21010-5. doi: 10.1073/pnas.1211150109.
654 46. Caramalho R, Tyndall JDA, Monk BC, Larentis T, Lass-Flörl C, Lackner M. Intrinsic
655 short-tailed azole resistance in mucormycetes is due to an evolutionary conserved aminoacid
656 substitution of the lanosterol 14α-demethylase. Sci Rep. 2017;7(1):15898. doi: 10.1038/s41598-
657 017-16123-9.
658 47. Young LY, Hull CM, Heitman J. Disruption of ergosterol biosynthesis confers resistance
659 to amphotericin B in *Candida lusitaniae*. Antimicrobial agents and chemotherapy.
660 2003;47(9):2717-24.
661 48. Luna-Tapia A, Willems HME, Parker JE, Tournu H, Barker KS, Nishimoto AT, et al.
662 Loss of Upc2p-inducible ERG3 transcription is sufficient to confer niche-specific azole
663 resistance without compromising *Candida albicans* pathogenicity. mBio. 2018;9(3):18. doi:
664 10.1128/mbio.00225-18.
665 49. Kelly SL, Lamb DC, Kelly DE, Manning NJ, Loeffler J, Hebart H, et al. Resistance to
666 fluconazole and cross-resistance to amphotericin B in *Candida albicans* from AIDS patients
667 caused by defective sterol delta5,6-desaturation. FEBS letters. 1997;400(1):80-2.
668 50. Kelly SL, Lamb DC, Kelly DE, Loeffler J, Einsele H. Resistance to fluconazole and
669 amphotericin in *Candida albicans* from AIDS patients. Lancet (London, England).
670 1996;348(9040):1523-4. doi: 10.1016/S0140-6736(05)65949-1.
671 51. Nolte FS, Parkinson T, Falconer DJ, Dix S, Williams J, Gilmore C, et al. Isolation and
672 characterization of fluconazole- and amphotericin B-resistant *Candida albicans* from blood of
673 two patients with leukemia. Antimicrobial agents and chemotherapy. 1997;41(1):196-9.

674 52. Robbins N, Collins C, Morhayim J, Cowen LE. Metabolic control of antifungal drug
675 resistance. Fungal genetics and biology : FG & B. 2010;47(2):81-93. doi:
676 10.1016/j.fgb.2009.07.004.
677 53. Kruger F. Trim Galore. A wrapper tool around Cutadapt FastQC to consistently apply
678 Qual Adapt trimming to FastQ files. 2015.
679 54. Corrochano LM, Kuo A, Marcet-Houben M, Polaino S, Salamov A, Villalobos-Escobedo
680 JM, et al. Expansion of signal transduction pathways in fungi by extensive genome duplication.
681 Curr Biol. 2016;26(12):1577-84. Epub 2016/05/31. doi: 10.1016/j.cub.2016.04.038. PubMed
682 PMID: 27238284; PubMed Central PMCID: PMCPMC5089372.
683 55. Langmead B, Salzberg SL. Fast gapped-read alignment with Bowtie 2. Nat Methods.
684 2012;9(4):357-9. Epub 2012/03/06. doi: 10.1038/nmeth.1923. PubMed PMID: 22388286;
685 PubMed Central PMCID: PMCPMC3322381.
686 56. Trapnell C, Roberts A, Goff L, Pertea G, Kim D, Kelley DR, et al. Differential gene and
687 transcript expression analysis of RNA-seq experiments with TopHat and Cufflinks. Nat Protoc.
688 2012;7(3):562-78. Epub 2012/03/03. doi: 10.1038/nprot.2012.016. PubMed PMID: 22383036;
689 PubMed Central PMCID: PMCPMC3334321.

690

Figure captions

Fig 1. sRNA hybridization and phenotypic analysis of 5-FOA-resistant epimutants. **(A)** sRNA hybridization of epimutants and revertants from an *rdrp3* mutant background, before (R – resistant) and after 5 (P5) or 10 (P10) passages without selection. P, *rdrp3*Δ parental strain (MU439). Blots were hybridized with antisense-specific probes against *pyrF*, *pyrG,* or 5S rRNA (loading control). **(B)** sRNA blot of epimutants and revertants from an *rdrp1* mutant background, before (R – resistant) and after 5 passages without selection (P5). P, *rdrp1*Δ parental strain (MU419). Blots were hybridized with antisense-specific probes against *pyrF*, *pyrG* or 5S rRNA (loading control). **(C)** Phenotypic analysis of one representative epimutant, before and after reversion. A *pyrF* epimutant (E2) is shown before and after 5 (P5) and 10 (P10) passages without selection, grown on MMC media, MMC supplemented with uridine and uracil, and MMC supplemented with 5-FOA, uridine, and uracil. *pyrG*$^{-}$, a known mutant of *pyrG,* served as a negative control; P, *rdrp3*Δ parental strain (MU439). **(D)** A *pyrG* epimutant (E4) is shown before and after 5 (P5) passages without selection, grown on MMC, MMC supplemented with uracil, and MMC supplemented with 5-FOA and uracil. P, *rdrp1*Δ parental strain (MU419).

Fig 2. 5-FOA resistance is associated with increased levels of sRNAs against either the *pyrF* or *pyrG* locus.

(A) Representative diagram of sRNAs mapped across the *pyrF* locus showing accumulation of both sense (- values) and antisense sRNA (+ values) in epimutant E1 (in red). Expression levels are greatly decreased in the revertant after 5 passages without selection (in blue). No increase in sRNA levels is seen in the surrounding regions. **(B)**

715 Representative diagram of sRNAs mapped across the *pyrG* locus showing accumulation
716 of both sense (+ values) and antisense sRNA (- values) in epimutant E4 (in red), with
717 greatly decreased sRNA levels in the revertant after 5 passages without selection (in
718 blue). No increase of sRNA levels is observed in the surrounding regions.

719

720 **Fig 3. Length and terminal nucleotide analysis of sRNAs in epimutants.**

721 Antisense sRNAs from epimutant strains and their corresponding revertants that map
722 against the *pyrF* and *pyrG* loci. **(A)** Analysis of the 5' nucleotide of antisense sRNAs that
723 map to the *pyrF* locus, isolated from the *pyrF* epimutant strain E1 and revertant. **(B)**
724 Analysis of the 5' nucleotide of antisense sRNAs that map to the *pyrG* locus, isolated from
725 the *pyrG* epimutant strain E4 and revertant. **(C)** Analysis of the size of antisense sRNAs
726 that map to *pyrF* in strain E1 and revertant. **(D)** Analysis of the size of antisense sRNAs
727 that map to *pyrG* in strain E4 and revertant.

728

729 **Fig 4. Epimutation decreases expression of *pyrF* and *pyrG* mRNA.**

730 **(A)** Expression of *pyrF* mRNA in *pyrF* epimutant and revertant strains (Passage 5, P5) as
731 determined through qRT-PCR, with actin expression used for the reference gene. Gene
732 expression levels were normalized relative to the *rdrp3*Δ parental strain (PS), using actin
733 as the reference gene via the comparative ΔΔCt method. N=3 experimental replicates;
734 error bars depict standard error of the mean (SEM). Significance determined via one-way
735 ANOVA (P=0.0005, F=13.37, 4 degrees of freedom) with post-hoc Tukey's Multiple
736 Comparison test. **(B)** Expression of *pyrG* mRNA in *pyrF* epimutant and revertant strains.
737 N=1. **(C)** Expression of *pyrF* mRNA in a *pyrG* epimutant and revertant strain as

738 determined through qRT-PCR, with actin expression used for the reference gene. Percent
739 expression was normalized relative to *rdrp1*Δ parental strain (PS). N = 3 experimental
740 replicates; error bars depict SEM. Significance determined via one-way ANOVA (P=0.51,
741 F=0.74, 2 degrees of freedom). **(D)** Expression of *pyrG* mRNA in *pyrG* epimutant and
742 revertant strain. N = 3 experimental replicates; error bars depict SEM. Significance
743 determined via one-way ANOVA (P=0.059, F=4.7, 2 degrees of freedom).
744

Supporting information

S1 Fig. *pyrF* and *pyrG* are differentially enriched for sRNAs in epimutant vs. revertant strains.

Genome-wide sRNA levels are plotted between two sequenced libraries, with values for one library plotted on the X and the other on the Y. The point representing *pyrF* is depicted in red and the *pyrG* is depicted in blue. E1 and E2 are *pyrF* epimutant strains; E4 is a *pyrG* epimutant strain.

S2 Fig. Epimutant revertants demonstrate a 5' uracil predominance in antisense sRNAs against *pyrF* and *pyrG*.

Analysis of the 5' nucleotide of antisense sRNAs that map to the *pyrF* and *pyrG* loci. Data from Fig. 3 is replotted here with an expanded y-axis to enable easier comparison of 5' terminal nucleotides in sRNA from revertant strains. **(A)** 5' terminal nucleotides of antisense sRNAs isolated from *pyrF* epimutant E1 and revertant. **(B)** 5' terminal nucleotides of antisense sRNAs isolated from *pyrG* epimutant E4 and revertant.

S3 Fig. A set of genes with discordant sRNA expression in epimutants vs. revertants are evenly distributed across the *Mucor* genome.

(A) Genome-wide sRNA levels are shown with the gene set that is expressed more than 15-fold higher in the E2 revertant than in the E2 epimutant shaded in red. That same gene set is also shaded in the comparison of the *rdrp1*Δ parent strain with the WT parent to

767 demonstrate that the same gene set is behaving anomalously in both comparisons. **(B)**
768 Genes with discordant sRNA expression are shown across the *Mucor* genome (red bars
769 not to scale relative to scaffold). These genes appear on every scaffold of the genome
770 that is greater than 41 kb in size.

771

772 **S4 Fig. Epimutant E7 maintains 5-FOA resistance after cessation of sRNA**
773 **expression.**

774 **(A)** The *pyrF* epimutant E7 maintains a degree of 5-FOA resistance even after 70
775 passages without drug selection (P70). An independent repeat of passaging
776 demonstrates continued 5-FOA resistance through 40 passages (P40v2). Strains were
777 grown on MMC media, MMC supplemented with uridine and uracil, and MMC
778 supplemented with 5-FOA, uridine, and uracil. P, *rdrp1*Δ parental strain (MU419). **(B)**
779 sRNA hybridization of passaged strains of epimutant E7. Epimutant E7 expresses sRNA
780 against *pyrF*, but this sRNA is no longer expressed from 15 passages (P15) through 70
781 passages (P70). Similarly, strains from an independent set of passages demonstrate no
782 sRNA against *pyrF* at passages 15 (P15v2), 30 (P30v2), or 40 (P40v2). The top portion
783 of the gel was stained with ethidium bromide (EtBr) to visualize the 5S rRNA loading
784 control, after which sRNA was transferred to a membrane for hybridization with an
785 antisense-specific probe against *pyrF.*

786 **S1 Table. Primers used in this study**

787 **S2 Table. Strains generated in this study**

788

Figure 1

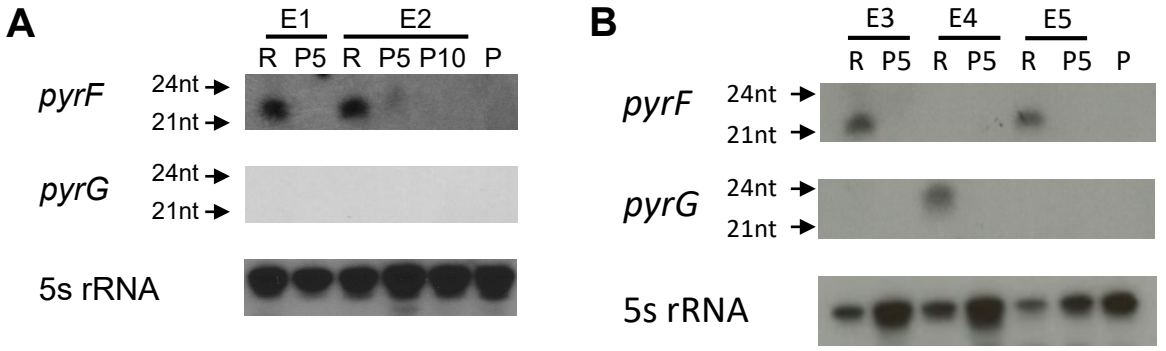
A
E1
E2
R P5 R P5 P10 P
pyrF
24nt
21nt
pyrG
24nt
21nt
5s rRNA
B
E3
E4
E5
R P5 R P5 R P5 P
pyrF
24nt
21nt
pyrG
24nt
21nt
5s rRNA

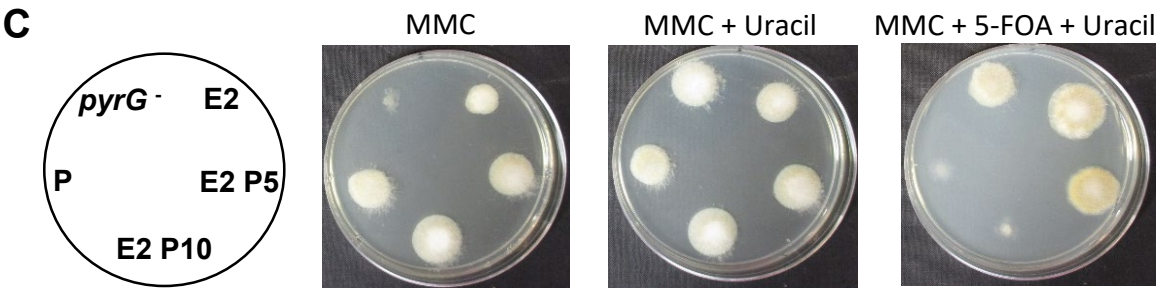
C
MMC
MMC + Uracil
MMC + 5-FOA + Uracil
pyrG -
E2
P
E2 P5
E2 P10

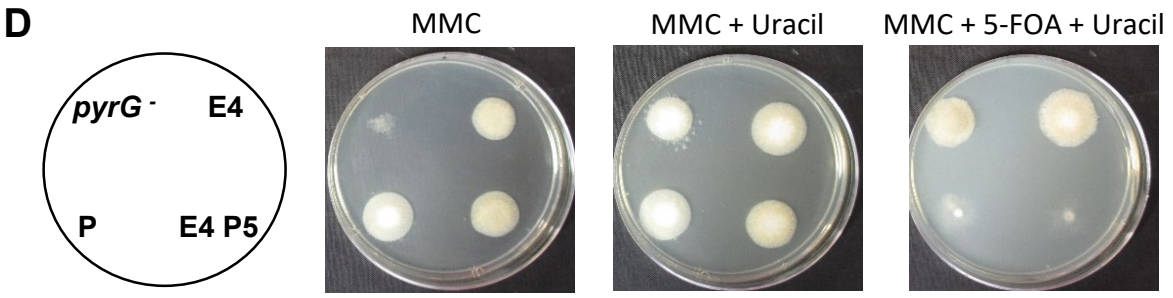
D
MMC
MMC + Uracil
MMC + 5-FOA + Uracil
pyrG -
E4
P
E4 P5

Figure 2

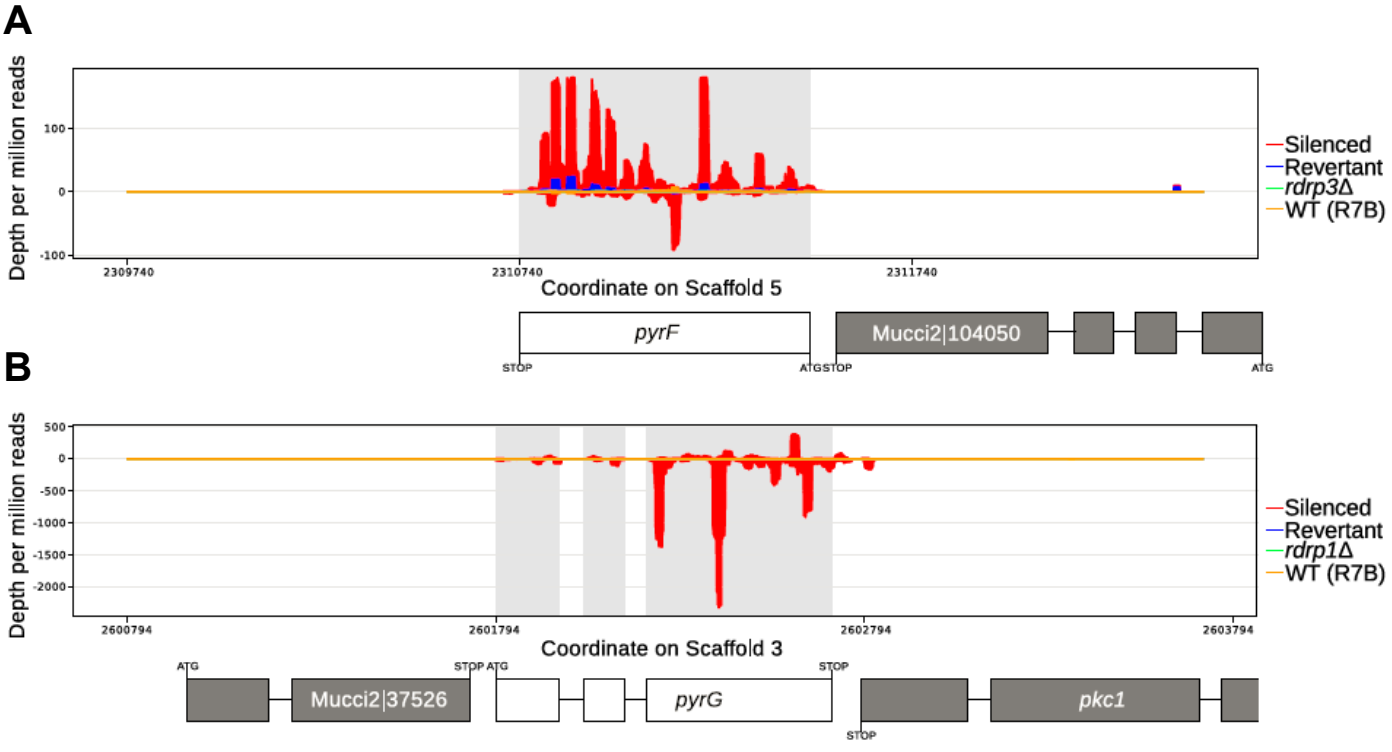
A
Depth per million reads
100
0
-100
2309740
2310740
2311740
Coordinate on Scaffold 5
Silenced
Revertant
rdrp3Δ
WT (R7B)
pyrF
Mucci2|104050
STOP
ATG
STOP
ATG
B
Depth per million reads
500
0
-500
-1000
-1500
-2000
2600794
2601794
2602794
2603794
Coordinate on Scaffold 3
Silenced
Revertant
rdrp1Δ
WT (R7B)
ATG
Mucci2|37526
STOP
ATG
pyrG
STOP
pkc1
STOP

Figure 3

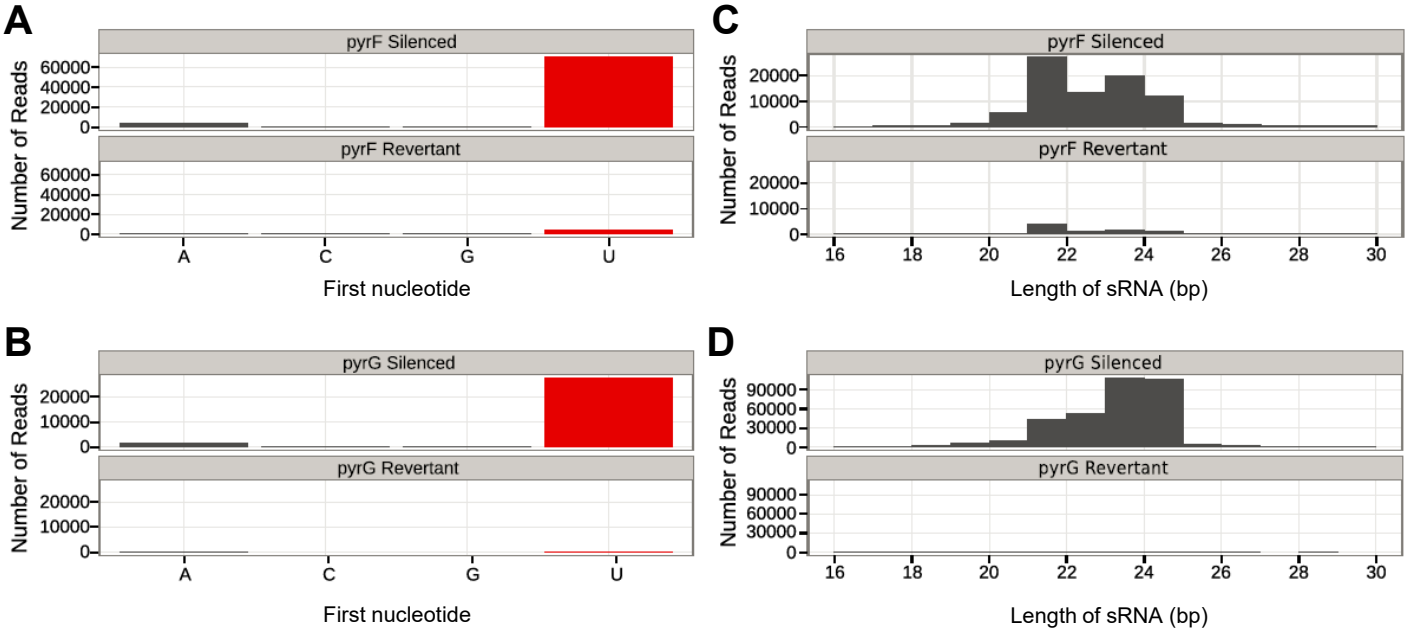
A
pyrF Silenced
pyrF Revertant
Number of Reads
60000
40000
20000
0
A
C
G
U
First nucleotide
C
pyrF Silenced
pyrF Revertant
Number of Reads
20000
10000
0
16
18
20
22
24
26
28
30
Length of sRNA (bp)
B
pyrG Silenced
pyrG Revertant
Number of Reads
20000
10000
0
A
C
G
U
First nucleotide
D
pyrG Silenced
pyrG Revertant
Number of Reads
90000
60000
30000
0
16
18
20
22
24
26
28
30
Length of sRNA (bp)

Figure 4

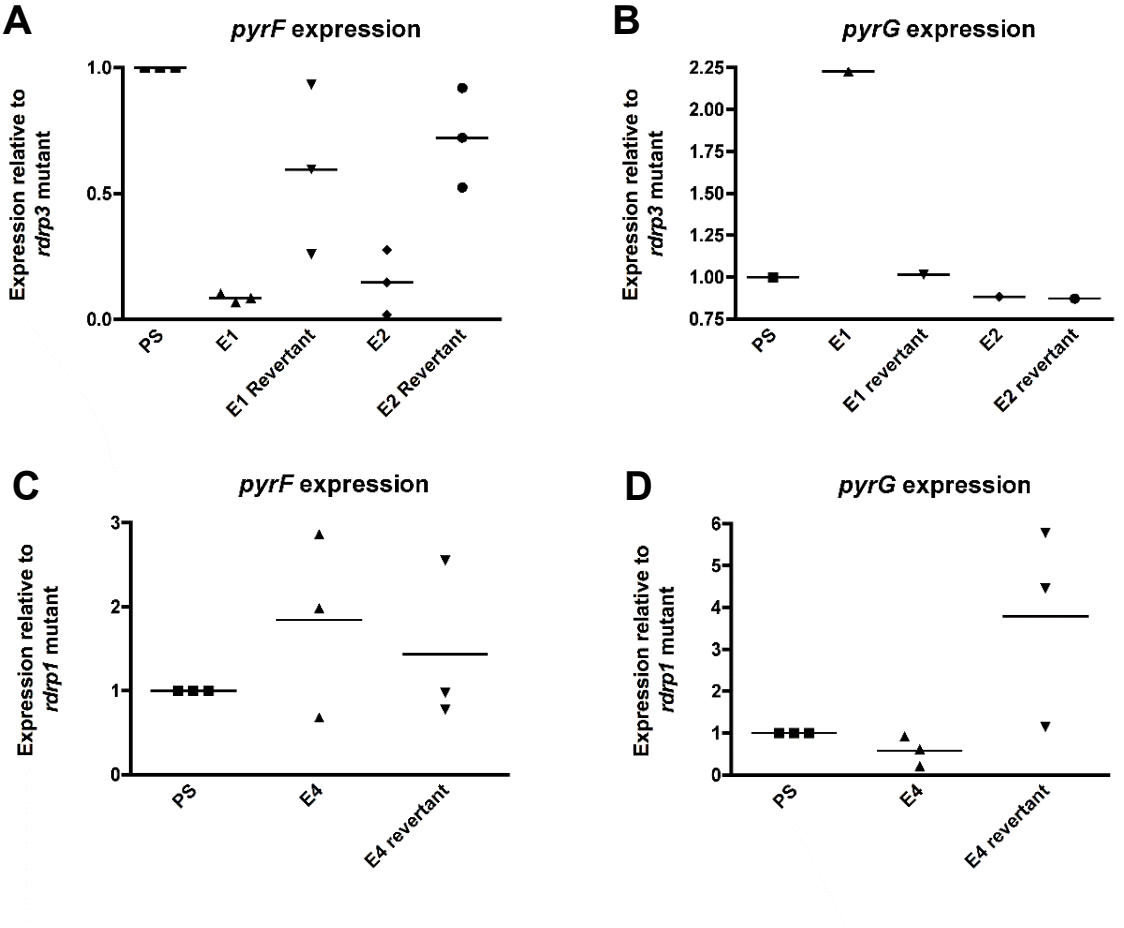
A
pyrF expression
Expression relative to rdrp3 mutant
1.0
0.5
0.0
PS
E1
E1 Revertant
E2
E2 Revertant
B
pyrG expression
Expression relative to rdrp3 mutant
2.25
2.00
1.75
1.50
1.25
1.00
0.75
PS
E1
E1 revertant
E2
E2 revertant
C
pyrF expression
Expression relative to rdrp1 mutant
3
2
1
0
PS
E4
E4 revertant
D
pyrG expression
Expression relative to rdrp1 mutant
6
5
4
3
2
1
0
PS
E4
E4 revertant